Oxygen-tuned magnetic coupling of Fe-phthalocyanine molecules to ferromagnetic Co films

D. Klar,[1,*] B. Brena,[2] H. C. Herper,[2] S. Bhandary,[2] C. Weis,[1] B. Krumme,[1] C. Schmitz-Antoniak,[1] B. Sanyal,[2] O. Eriksson,[2] and H. Wende[1]

[1]*Faculty of Physics and Center for Nanointegration Duisburg-Essen (CENIDE), University of Duisburg-Essen, Lotharstraße 1, D-47048 Duisburg, Germany*

[2]*Department of Physics and Astronomy, Uppsala University, Box 516, 751 20 Uppsala, Sweden*

(Received 17 September 2013; revised manuscript received 11 December 2013; published 30 December 2013)

The coupling of submonolayer coverages of Fe-phthalocyanine molecules on bare and oxygen-covered ferromagnetic Co(001) films was studied by x-ray-absorption spectroscopy, especially the x-ray magnetic circular dichroism, in combination with density functional theory. We observe that the magnetic moments of the paramagnetic molecules are aligned even at room temperature, resulting from a magnetic coupling to the substrate. While the magnetization of the Fe ions directly adsorbed on the Co surface is parallel to the magnetization of the Co film, the introduction of an oxygen interlayer leads to an antiparallel alignment. As confirmed by theory, the coupling strength is larger for the system FePc/Co than for FePc/O/Co, causing a stronger temperature dependence of the Fe magnetization for the latter system. Furthermore, the calculations reveal that the coupling mechanism changes due to the O layer from mostly direct exchange to Co of the bare surface to a 180° antiferromagnetic superexchange via the O atoms. Finally, by comparing the experimental x-ray-absorption spectra at the N K edge with the corresponding calculations, the contribution of the individual orbitals has been determined and the two inequivalent N atoms of the molecules could be distinguished.

DOI: 10.1103/PhysRevB.88.224424 PACS number(s): 33.15.Kr, 33.55.+b, 71.15.Mb, 78.70.Dm

I. INTRODUCTION

The rapid progress of the information technology has caused the continuous downscaling of electronic and magnetic devices. To avoid reaching the size limit of conventional techniques, one has to develop novel alternatives. Organic spintronic devices are a potential realization for such alternative applications.[1–4] The challenge for an industrial usage is the control of the magnetization. The paramagnetic porphyrin molecule with a metallic ion in the center was reported to be a promising candidate.[5–8] The magnetization of these planar molecules can be controlled by a ferromagnetic (FM) film. Not only the exchange coupling, but the spin state of iron porphyrin molecules may be tuned by physisorption[9,10] or chemisorption on substrates.[11]

A metal phthalocyanine (Pc), investigated in this work, differs from the porphyrin in the local surrounding of the central ion. In the porphyrin molecule, there are only four N atoms that bind with equivalent distance to the central ion. In the Pc molecule there are additionally four N atoms without bonds to the central ion [N_b, Fig. 1(a)]. Pc molecules have no out-of-plane ligands, which enables them to lie perfectly plane on a surface, including also the carbon atoms, which enhances the surface-molecule interaction. Betti *et al*. showed a long-range structural ordering of FePc on Au(110) and a strong influence of the surface on the electronic properties of the molecules.[12] The modified ligand field influences the electronic properties of the Fe ion, while maintaining the paramagnetism. Pc molecules are topic of several areas of research and applications, e.g., organic solar cells.[13,14] With x-ray-absorption spectroscopy (XAS) and x-ray magnetic circular dichroism (XMCD), a magnetic coupling between CoPc and an Fe substrate has already been seen by Annese *et al*.[15] and very recently the coupling was also demonstrated between FePc and a Co substrate.[16] Cinchetti *et al*. obtained an efficient spin injection of a Co surface into Cu-phthalocyanine molecules, but did not focus on the magnetic coupling between the ferromagnet and the molecules.[17] Single molecule magnets, composed of two parallel phthalocyanine rings and a Tb ion in between, were recently studied with XAS and XMCD, showing butterfly hysteresis[18] on a gold substrate at $T = 2$ K and antiferromagnetic coupling (AF) on thin Co and Ni films up to $T = 100$ K.[19,20] While the Tb ion is separated from the surface by the Pc ring and the exchange coupling between the Tb and the FM substrate is only via the ligand, the Fe in the FePc molecule is in direct contact with the surface, as we show below.

In this work we investigate in which way the change of the ligand field, compared to porphyrin molecules, modifies the electronic and magnetic properties of the Fe ion. We studied *in situ* prepared samples with submonolayers of FePc molecules on a ferromagnetic Co(001) film with and without oxygen between the film and the molecules with the element-specific XAS and XMCD. The Fe ion in the center of the plane molecule is stable in the Fe(II) oxidation state. The thin films of Co exhibit a remanent magnetization parallel to the surface, offering the opportunity to measure the magnetic signal without an applied field.

In the literature various works on the fcc(111) surfaces (Ag, Cu, Au) exist.[21–32] In these works the structure and the exchange mechanisms are studied. Since a different surface is investigated in the present work, it is not surprising that we find different adsorption sites. From our investigations it turned out that the coupling mechanism and adsorption position strongly depend on the choice of the molecular substrate hybrid system. The focal point of the analysis is the demonstration of the possibility to tailor the magnetic coupling by oxygen in the case of FePc on Co(001). By combining the experimental investigations with state-of-the-art density functional theory, we can describe the coupling mechanism on both surfaces and gain insight into the local magnetic structure of molecule and surface. We calculate the angle-dependent XAS at the N K

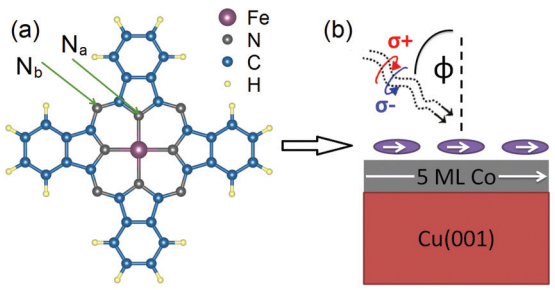

FIG. 1. (Color online) (a) Sketch of the FePc molecule which is composed of an Fe (purple) ion in the center, 8 N (gray), 32 C (blue), and 16 H (yellow) atoms. (b) Schematic illustration of the XMCD measurement for the sample FePc/Co/Cu(001) under the incidence angle ϕ.

edge and we are able to separate the contributions of the two inequivalent N atoms, the ones with and the ones without bonding to the Fe ion. Furthermore the calculations give some indication of the preferred adsorption site and electronic structure on the two surfaces.

II. EXPERIMENTAL METHODS

The samples were prepared *in situ* at a base pressure of 10^{-10} mbar. As cleaning procedure for the Cu(001) surface we carried out several sputter-heating cycles. The purity of the surface was checked with low-energy electron diffraction and Auger electron spectroscopy. Using electron-beam evaporation we produced an epitaxial ferromagnetic Co film with a well-defined thickness of 5 monolayers (MLs) and the easy axis of magnetization parallel to the surface.[33] During the growth of the film the thickness was controlled by monitoring oscillations in the medium-energy diffraction pattern. The deposition rate was 1 ML/min. To achieve the oxygen-covered Co film, an oxygen $(\sqrt{2} \times 2\sqrt{2})R45^\circ$ superstructure was constructed on the Cu single crystal. The oxygen atoms act as a surfactant for the growth of the Co film and this results in a well-characterized $c(2 \times 2)$ superstructure of 0.5-ML atomic oxygen on top of the Co film.[34–37] The easy axis of the Co film remains unchanged in the presence of the oxygen coverage. A submonolayer of Fe(II)Pc molecules was thermally deposited from a Knudsen cell onto the substrate held at room temperature. The evaporation rate of about 0.05 MLs/min was controlled during the deposition with a microbalance fixed on the top of the evaporator. All molecules adsorb intact and flat on the surface, meaning that the Pc plane is parallel to the surface (experimental characterization in Secs. III and VI).

The XAS measurements in total electron yield were performed at the undulator beamline UE52-SGM at HZB-BESSY II. With the element-specific XAS and XMCD techniques at the Co and Fe $L_{2,3}$ edges and the N K edge, we analyzed the electronic and magnetic properties. One of our focal points is the study of the magnetic coupling between the Fe ion and the ferromagnetic Co film. Since the magnetization of the Co film is parallel to the surface in both cases, i.e., with and without oxygen surfactant, the XMCD measurements were done at grazing incidence ($\phi = 70^\circ$). Angle-dependent XAS at the N K edge and Fe $L_{2,3}$ edges with linearly polarized light were carried out to study the orientation of the FePc molecules on the surface and contribution of the different orbitals. The XMCD measurements were performed in an applied field of 20 mT parallel to the beam. This small magnetic field serves only to saturate the in-plane magnetization of the ferromagnetic Co film. To avoid radiation damage to the molecules, we performed the measurements at a reduced x-ray intensity. We also moved the sample frequently, so that the x-ray spot impinges on a fresh position.

III. COMPUTATIONAL METHODS

The electronic and magnetic structures of FePc on bare and $c(2 \times 2)$O/Co(001) have been determined from density functional theory (DFT) calculations using the VASP code[38] and the projector augmented wave approach (PAW).[39] The localized character of the 3d orbitals was taken into account by the GGA + U approach. The effective $U_{\text{eff}} = U - J$ value used in the method of Dudarev[40] has been chosen to be 3 eV, which has been proven to give accurate results and is nowadays commonly used for this system.[41,42] van der Waals forces were incorporated using Grimme's second method as implemented in VASP. [43] The molecule-substrate system was modeled by a 3-ML-thick Co film in a $(25.527\ \text{Å})^3$ supercell with one FePc molecule on top. For the oxidized surface, 1/2 ML of oxygen was added which leads, in agreement with the experiment, to a $c(2 \times 2)$ reconstruction of the Co(001) surface. The calculated height of the O atoms above the first Co layer was 0.83 Å which is close to the value observed for a $c(2 \times 2)$ O/Ni(001) surface.[44] In order to determine the ground-state configuration, the molecule was placed on top, bridge, and hollow site positions with Fe-N bonds parallel to the substrate axis and 45° rotated relative to the axis. Except for the bottom Co layer, all atoms were allowed to relax until the forces are smaller than 0.02 eV/Å. All calculations have been performed with a plane-wave cutoff of 400 eV and a Γ-point only k mesh. Only for the determination of the exchange energy, a $3 \times 3 \times 3$ mesh was adopted. The comparison of the experimental results with the theoretical near-edge absorption fine-structure (NEXAFS) of the distorted molecule, cut out from the VASP optimization, are used to investigate the effect of the loss of symmetry on the absorption spectra.

The near-edge absorption fine-structure (NEXAFS) calculations were carried out for a single FePc molecule using the DFT code StoBe (Ref. 45) with the transition potential approach, which means that the core hole was described by a half filled N 1s core orbital. The structure of the gas phase molecule had previously been energy optimized at the B3LYP/DFT level, as described in Ref. 46. For the N K-edge spectra, we have used the generalized gradient corrected exchange functional by Becke[47] and the correlation functional by Perdew.[48] The igloo-iii triple ζ basis of Kutzelnigg, Fleischer and Schindler[49] was employed for describing the core excited N atom, while the remaining N atoms were represented by effective core potentials of five electrons provided by the StoBe package. For the other atoms, triple ζ plus valence polarization basis sets provided by the StoBe package were used. In addition, a double basis set technique is used by StoBe to minimize the energy, as well as an augmented diffuse

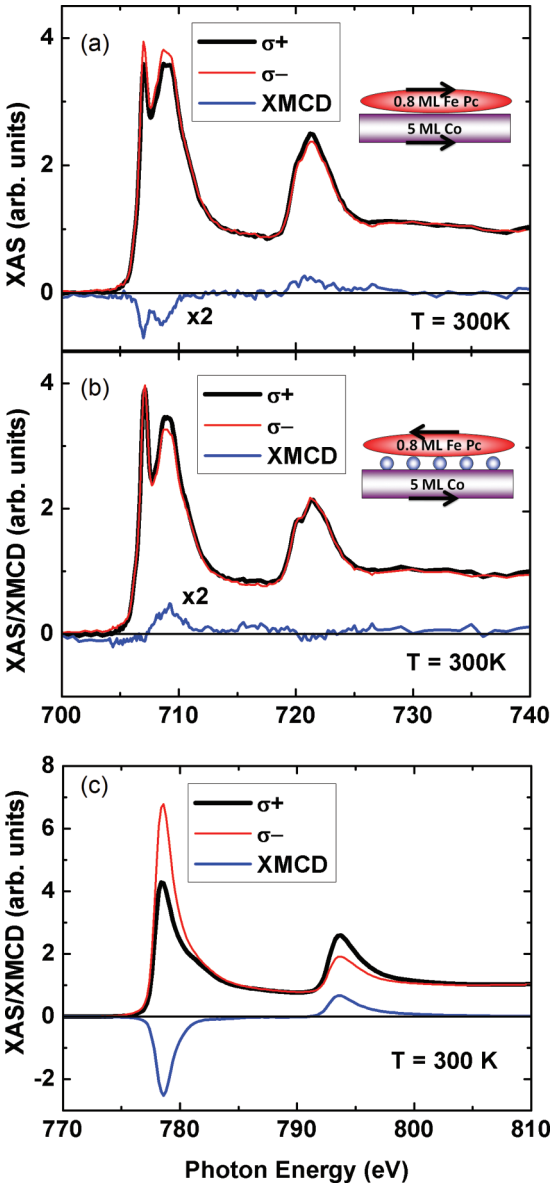

FIG. 2. (Color online) Fe $L_{2,3}$ XAS and XMCD spectra of 0.8-ML FePc/5-ML Co (a), 0.8-ML FePc/O/5-ML Co (b) and Co $L_{2,3}$ XAS and XMCD spectra (c). The spectra are recorded at room temperature and with a grazing angle of $\phi = 70^{\circ}$.

basis set (19s, 19p, 19d) to calculate the excitation energies and the transition moments.[50] The angle-resolved spectra of the N K edge were obtained as the average of the spectra of each of the two nonequivalent N atoms in the molecule, which are the pyrrole (N_a, Fig. 1) and the aza-bridge nitrogens (N_b, Fig. 1). Each single N spectrum was aligned to the related ionization potential (IP) calculated with the Δ KS approach. The simulated spectra were convoluted with Gaussian curves of full width at half maximum (FWHM) of 0.5 eV up to the IP, linearly increasing to 8.0 eV for an interval of 50 eV, and constant above. The spectra were moreover shifted by 0.7 eV, which include the relativistic corrections for the N atoms.[51]

The two theoretical contributions have different aims, since the programs used have different capabilities. We have used the VASP calculations to accurately determine the adsorption site

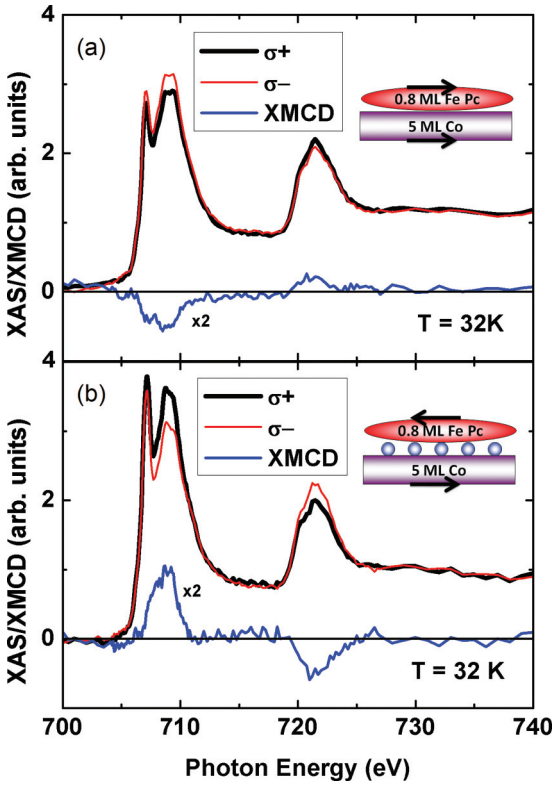

FIG. 3. (Color online) Fe $L_{2,3}$ XAS and XMCD spectra of 0.8-ML FePc/5-ML Co (a), 0.8-ML FePc/O/5-ML Co (b) measured at $T = 32$ K and with a grazing angle (ϕ) of 70°.

for the molecule plus substrate. StoBe N K-edge calculations were performed instead with the aim to understand the molecular orbital origin of the absorption peaks, which could confirm the strong bonding between the molecule and the surface. With this approach we have been able to consider only the distortion of the molecule induced by the chemisorption, and we have excluded the substrate.

IV. MAGNETIC COUPLING BETWEEN MOLECULE AND SUBSTRATE

The XA spectra and the XMCD at the Fe $L_{2,3}$ edges on the bare (a) and on the oxygen-covered (b) Co film show distinct characteristics; see Figs. 2(a) and 2(b). The XAS is normalized to match 0 before the L_3 edge and 1 after the L_2 edge. The three spectra in this figure were recorded at room temperature (300 K). The photon incidence angle ϕ was 70° to the optical axis [Fig. 1(b)]. In the spectra the red line (σ^-) represents the normalized spectrum for left circularly polarized light, the black one (σ^+) is for right circularly polarized light, and the blue line is the difference ($\sigma^+ - \sigma^-$). The Fe XMCD signal is amplified by a factor of 2 for a clearer presentation. At the Fe L_3 edge one can see a double structure with a very sharp peak at 707.1 eV and a broader one at 708.9 eV. The intensity relation of these two peaks differs slightly for the two unequal surfaces. While the heights of the two peaks are almost equal in the case of the bare Co surface, the sharp peak is clearly higher than the broader one for the O-covered surface. The signs of the XMCD signals at the Fe and Co L_3

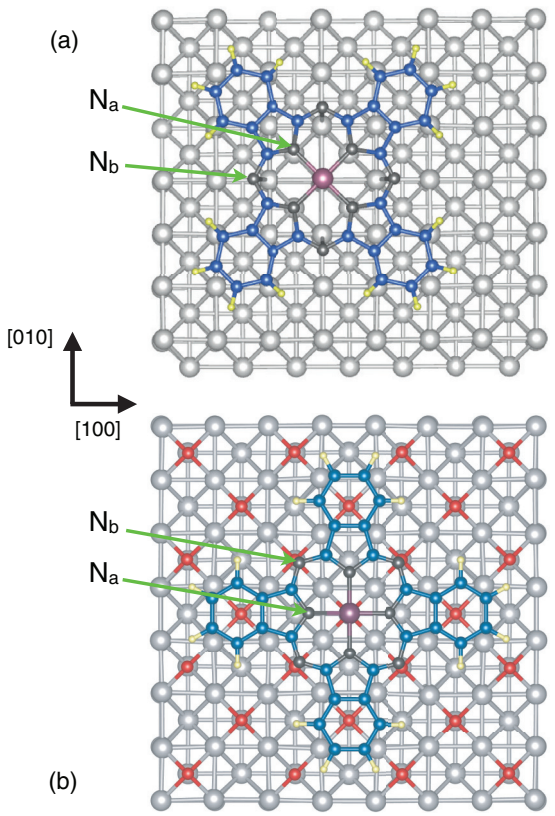

FIG. 4. (Color online) (a) Top view of the ground-state configuration of FePc/Co(001) [note that the long axis of the FePc molecule is rotated with 45° with respect to the (100) direction of the substrate]. The purple sphere represents the Fe atom, dark grey spheres represent the N atoms, blue spheres the C atoms, yellow spheres the H atoms, and light grey spheres the Co atoms. (b) Top view of the ground-state configuration on FePc on $c(2 \times 2)$O/Co(001). Red circles denote O atoms. The color scheme for the other atoms is the same as in (a).

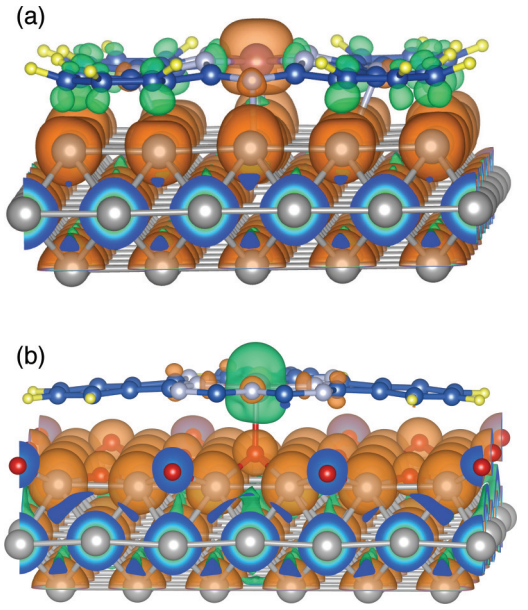

FIG. 5. (Color online) Isosurface spin density close to the Fermi level for FePc on top 45° site on bare Co(001) (a) and on top of O position in case of oxidized surface (b). Brown denotes up-spin and green down-spin density such that the same color of magnetization density of Fe and Co surface (a) corresponds to FM coupling whereas the different colors on the oxidized surface (b) denote an AF coupling of Fe and Co.

edges [Fig. 2(c)] are the same for FePc/Co/Cu(001) [Fig. 2(a)], but opposite for the molecules on the O interlayer [Fig. 2(b)]. This indicates ferromagnetic coupling between molecule and substrate in the case of a direct contact between Fe and Co and an antiferromagnetic coupling for the oxygen-covered surface. Furthermore, on the O-covered film the XMCD signal is smaller than on the bare film. Besides, only the broader feature at the L_3 edge contributes to the dichroic signal for FePc/O/Co/Cu(001). The fine structures in the XAS hardly change with temperature. However, the XMCD intensity for the case with the intermediate oxygen layer exhibits a clear temperature dependence indicating a weaker magnetic coupling; cf. Figs. 2 and 3.

These findings are supported by the DFT calculations that show that the FePc molecule on the bare Co substrate is adsorbed on top of Co with a rotated geometry of 45° (as described in the caption of Fig. 4), whereas on the oxidized surface the ground state is adsorbed at the top of the O position, see Fig. 4, without rotation. In both cases the lateral orientation of the molecule is such that the N_a-type nitrogen atoms sit on top of Co atoms. On Co(001) the Fe-N_a bond length is increased by 0.02 Å compared to FePc on the oxidized surface or in gas phase (calculated under the same conditions). Also the angle between C-N_a-C is reduced by about 4°. This means that the deformation of the molecule is stronger due to the stronger bonding to the substrate layer. These findings hint to a change in the crystal field compared to the molecule on the oxidized substrate. For more structural details we refer to Ref. 52. Furthermore, the adsorption site on Co(001) is different from the findings of Javaid *et al.* who observed a bridge position in the case of MnPc on Co(001).[53] However, from their paper it is not clear whether they have included 45° rotated configurations. Furthermore, the spin state of Mn is different which may also lead to a preference of the bridge position. The different adsorption positions do not affect the spin state. In both cases the molecules are in an $S = 1$ spin state and the Fe atom carries a magnetic moment of $2\mu_B$. However, the coupling to the surface becomes quite different with O. In agreement with the experimental findings, the magnetic coupling changes from FM to AF if an O adlayer is included; see Fig. 5. The sign change is accompanied by a reduction of the coupling strength. On the bare Co substrate, the coupling between molecule and surface obtained from the magnetic force theorem amounts to 0.229 eV whereas on the oxidized surface, the magnitude of coupling is reduced by a factor of 2, namely to −0.097 eV. The reduction of the magnetic coupling is in line with the strong temperature dependence of the XAS and XMCD spectra at the Fe $L_{2,3}$ edges for 0.8-ML FePc in the presence of an O adlayer, cf. Figs. 2 and 3. Compared to the dichroic signal at room temperature, the XMCD has increased at 32 K, especially for FePc/O/Co/Cu(001). The stronger temperature dependence indicates weaker interaction between molecule and substrate caused by the O adlayer. On the bare Co film the Fe ion interacts directly with the

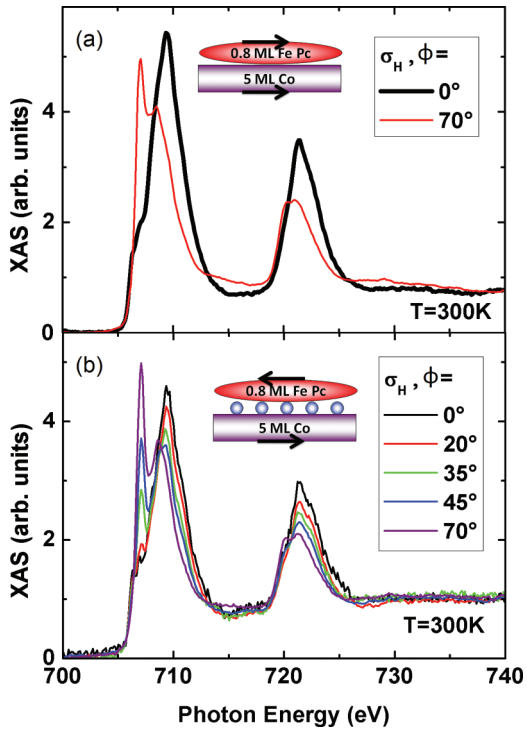

FIG. 6. (Color online) Angle-dependent Fe $L_{2,3}$ XAS spectra of 0.8-ML FePc/5-ML Co (top), 0.8-ML FePc/O/5-ML Co (bottom) measured with linear horizontal polarized x rays.

film, leading to a strong ferromagnetic coupling with a weak temperature dependence of the Fe XMCD signal.

Hence, the preferred adsorption site changes with O, since the coupling mechanism between molecules and the substrate on the oxidized surface is also different from the coupling on the bare Co substrate. On the bare Co surface, a direct coupling between the Fe atom and the Co atom underneath is observed, which can be seen from the magnetization density in Fig. 5(a). However, not only the Fe but also the C atoms in the benzene rings possess a magnetization perpendicular to the plane of the surface, albeit the moments of the C atoms are small, whereas the magnetization density of the N atoms is mostly directly in the plane of the molecule. Consequently, on the bare Co substrate a mixture of direct coupling and indirect coupling via the benzene rings occurs. This fact stresses the important role of the benzene C atoms in the FePc coupling to the Co surface. In contrast to FePc on Co(001), the C atoms of the benzene rings play a minor role in case of the oxidized surface; see Fig. 5(b). The magnetic coupling between molecule and surface is mainly mediated by the coupling of the Fe atom to the Co atom in the second layer via the O atom, i.e., the dominating mechanism is a 180° superexchange. The pyrrole and benzene rings show only small coupling effects with the surface. Only C atoms next to N_b atoms exhibit magnetization perpendicular to the surface. The N_a atoms interact mainly with the central Fe atom.

The spectra of the angle-dependent measurements with linear horizontal polarized x rays at the Fe $L_{2,3}$ edges show strong linear dichroism; see Fig. 6. This confirms the known orientation of the Pc molecules lying flat on the surface.[54] This fact is also underpinned by the N K-edge spectra discussed in Sec. VI. The spectra at the Fe $L_{2,3}$ edges have been recorded for two (five) photon angles in the case of the bare (oxidized) Co substrate; see Fig. 6. In both cases a detailed angular dependence is observed. For grazing incidence angles there is a clear double structure. For $\phi = 70°$ the sharp peak at the left side of the L_3 edge is even more intense than the broad one. With decreasing angles, the intensity of the first peak also decreases such that for 20° and 0° it is hardly visible. The structures are sharper for the molecules on the O-covered film and the spectra look more like those of the free molecule, implying once more a weak interaction.

V. CALCULATED MAGNETIC STRUCTURE

The projected spin moment of the ground state of FePc on Co(001) is $2\mu_B$ and the molecule is in an intermediate spin configuration with an $S = 1$ spin state. This seems on the first glance to contradict previous findings for the Fe porphyrin molecule on Co(001) where the oxygen was reported to stabilize a high-spin state.[7] But in that paper[7] only one single oxygen atom was used, which acts as a ligand whereas the whole oxygen layer used in the present work screens the interaction with the surface but no isolated Fe-O ligand appears. The $S = 1$ spin state found here is in agreement with previous calculations for FePc on the bridge position.[41] The N_a atoms directly bound to the Fe have a spin moment of $-0.02\mu_B$, while the N_b atoms have a spin moment of $0.023\mu_B$. Small spin moments are also obtained for some of the C atoms in the benzene rings. More specifically, the eight more external C atoms have a spin moment of $-0.016\mu_B$, and the eight atoms directly bound to these and still belonging to the benzene rings have a spin moment of $-0.034\mu_B$. Due to the particular distortion of the adsorbed molecule, these atoms are at rather short bonding distances from the Co atoms underneath, of 2.01 Å and 2.16 Å respectively. This result further strengthens the observation that in FePc, the outer C atoms in the benzene rings participate in the hybridization with the Co surface.

The calculated density of states for the chemisorption configuration on top of Co 45° is shown in Fig. 7(a). The electronic configuration is a $(d_{xy})^2$ $(d_{z^2})^2$ $(d_\pi)^2$, which also corresponds to one of the two proposed configurations for the FePc molecule in the gas phase; see for example Ref. 55. Compared to gas phase density of states, the d peaks are broader due to interaction with the surface. [41]

As discussed in Sec. IV, the spin state and the magnetic moments of the Fe atom are not changed in the presence of an O adlayer. The electronic structure shown in Fig. 7(b) corresponds to a $(d_{xy})^2$ $(d_{z^2})^1$ $(d_\pi)^3$ configuration. This configuration is according to Ref. 55, one possible electronic configuration for FePc. The other one is the $(d_{xy})^2$ $(d_{z^2})^2$ $(d_\pi)^2$ configuration obtained on the bare Co(001) substrate.

Analogous to FePc on Co(001), small spin moments of about $0.02\mu_B$ occur at the N_a atoms for the oxygenated system. Furthermore, the oxygen atom directly beneath the Fe atom carries a spin moment of $0.18\mu_B$ which corresponds approximately to the average spin moment of all O atoms on the surface. A strong hybridization between O s and p states [gray shaded areas in Fig. 7(b)] with d_π and d_{z^2} states of Fe is observed; see Fig. 7(b). The FM coupling

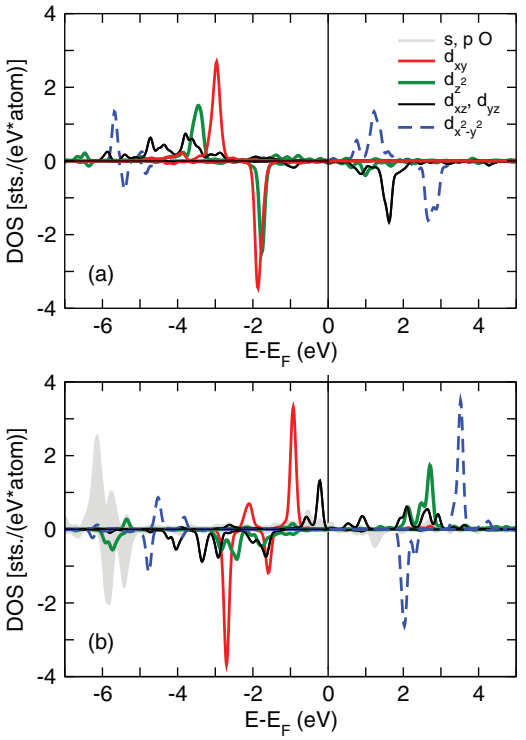

FIG. 7. (Color online) (a) Projected density of states (DOS) of the Fe *d* orbitals in the FePc/Co(001) top 45° adsorption site. (b) DOS of the Fe *d* orbitals in FePc/$c(2 \times 2)$O/Co(001) top of O adsorption site. Gray shaded areas mark the *s* and *p* density of states of the O atom beneath the Fe atom.

between O and Co atoms on the $c(2 \times 2)$O/Co(001) surface has already been reported previously by Sorg *et al.*[36] However, the size of the induced moments is slightly smaller than in the present paper being related to the fact that they used a smaller muffin-tin sphere for the projection of the magnetic moment.

Compared to the free molecule and the bare O/Co(001) surface, the magnetic moments of the Fe atom and O atom underneath are increased by $0.04\mu_B$ and $0.02\mu_B$, respectively, whereas the moment of the Co atom in the first Co layer is reduced by $0.05\mu_B$. This hints to a strong interaction between FePc and the Co substrate via the O atoms. However, changes in the magnetic structure of the surface are not restricted to atoms of the direct Fe-O-Co bond. The molecule leads to a reduction of the O moments under the pyrrole and benzene rings compared to the FePc free surface where the average O moment amounts to $0.17\mu_B$; see Fig. 8(b) for more details. This reduction in moment is continued in the first Co layer which also shows considerably reduced moments of $1.4–1.7\mu_B$ (the average moment without FePc is $1.75\mu_B$) in the same regions. Only Co atoms being nearest neighbor to Fe have higher moments of $1.85\mu_B$; see Fig. 8(a). Without the O layer, the magnetic structure of the Co surface is only changed locally, i.e., only Co atoms directly under the molecule show a variation of the magnetic moment. The Co atom, which directly couples to the Fe atom, has a magnetic moment of $2.01\mu_B$ whereas the Co atoms under the benzene rings have smaller moments between $1.5–1.7\mu_B$. All other Co

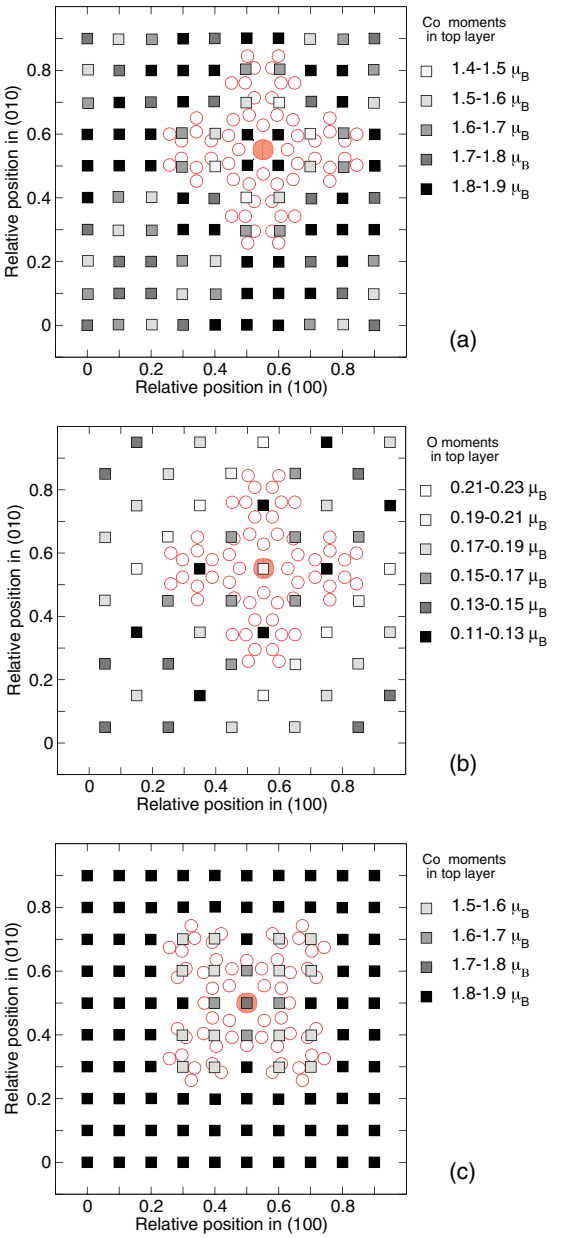

FIG. 8. (Color online) Profile of the magnetic moments in the first Co layer (a) and in the O adlayer (b) in presence of the FePc molecule on O/Co(001). Profile of the magnetic moments in the first Co layer on the bare Co(001) substrate (c). The position of the molecule is sketched by red circles.

atoms in the surface layer possess magnetic moments between $1.8\mu_B$ and $1.9\mu_B$; see Fig. 8(c). A similar reduction of the magnetic moment of the Co substrate in the vicinity of the Pc molecule has been observed by Chen and Alouani for CoPc on Co(111).[28]

Since the influence of the molecule on the magnetic moments of the surface seems to be quite short ranged on the Co(001) [Fig. 8(c)], the strong oscillations in magnitude in the case of FePc on O/Co(001) are not only caused by the molecule, which is weakly bonded to the surface, but are mostly due to the $c(2 \times 2)$ reconstruction of the surface.

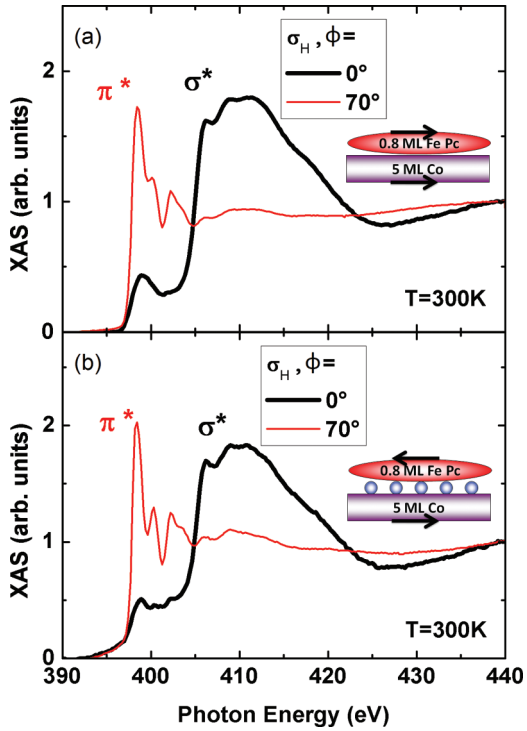

FIG. 9. (Color online) Angle-dependent N K XAS spectra of 0.8-ML FePc/5-ML Co (a), 0.8-ML FePc/O/5-ML Co (b) measured with linear horizontal polarized x rays.

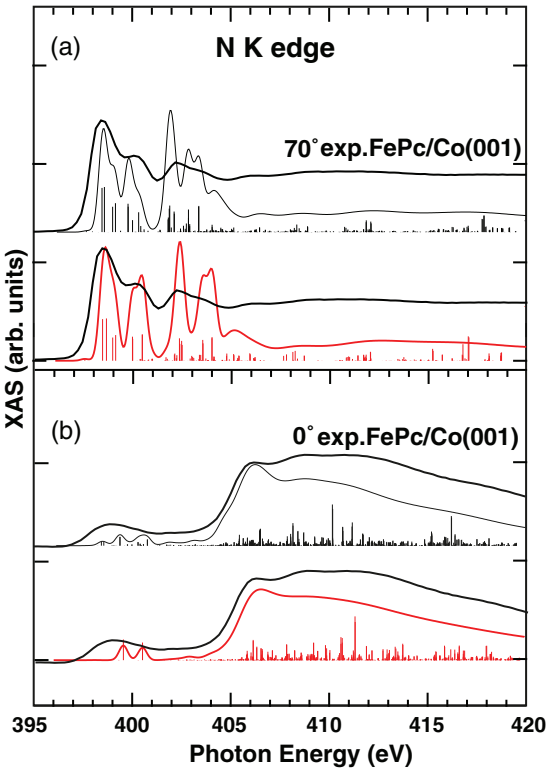

FIG. 10. (Color online) N K-edge experimental and theoretical spectra. (a) Quasiperpendicular (70°). (b) Parallel (0°) polarization. The experimental spectrum for the case without an intermediate layer of atomic oxygen is shown as the black thick line, the black thin line is the total calculated spectrum for the relaxed FePc, and the red line is the total spectrum for the symmetric FePc. The bar graphs show the calculated oscillator strengths (red bars represent the symmetric FePc and black bars the relaxed FePc).

VI. N K-EDGE NEXAFS

In order to gain additional information regarding the relative orientation of the molecule and substrate and the interaction with the surface, we studied N K-edge XA spectra. The investigation of the K-edge NEXAFS with linearly polarized x rays has the advantage that the so-called "search-light effect" can be used in its full strength. For the case of the nitrogen K edge the electron is excited from the initial nitrogen 1s state into final (unoccupied) p states. The direction of the electric-field vector acts as a search light for this excitation. If the electron is excited into the direction of the molecular plane, the unoccupied σ^*orbitals are probed. The asymmetric line shape of these resonances can be described in a scattering framework (see, e.g., Ref. 56). However, if the electric-field vector is perpendicular to the molecular plane, the unoccupied π^* resonances are probed. Hence, if the NEXAFS spectra exhibit a strong polarization dependence, the orientation of the molecules on the surface can be analyzed. Furthermore, the fine structures in the NEXAFS spectra provide insight into the interaction of the molecule with the surface. In an earlier work we could demonstrate that an intermediate layer of atomic oxygen leads to an effective decoupling of the nitrogen atoms in Fe-porphyrin molecules from the substrate.[7] Because of the weaker interaction of the nitrogen atoms with the surface, sharper features in the nitrogen K-edge NEXAFS have been detected for the case of Fe-porphyrin molecules adsorbed on the oxygen layer.[7] We will inspect if a similar effect is also seen for the Fe-phthalocyanine molecules studied here.

Polarization-dependent N K-edge measurements of organic conjugated molecules are especially sensitive to the π^* molecular orbitals close to the energy gap, and can therefore provide unique information about molecular structure and intermolecular interactions. We have performed N K-edge NEXAFS measurements and theoretical simulations for radiation with electric field parallel (0°) and almost perpendicular (70°) to the surface; see Fig. 9. The experimental spectra indicate that the molecules are oriented flat on the Co surface. In Fig. 10 we compare the experimental N K-edge measurements to the computed spectra for the single molecule obtained for a FePc with D_{4h} symmetry, and for the relaxed on top 45° FePc resulting from the geometry relaxation on the bare Co surface presented in Fig. 4(a). We start our analysis from the spectra obtained for the perpendicular polarization of Fig. 10(a). The curves computed for both cases (D_{4h} symmetric, red thin curve, and distorted molecule, black thin curve) have an overall similar structure. The small variations in the peak positions and intensities reflect the changes in the π^* molecular structure due to the distortion of the geometry. Two major experimental π^* resonances at the almost perpendicular polarization at 70° are found at about 398.5 eV and at 400.3 eV followed by a deep valley at 401.3 eV and by a series of indistinguishable peaks at 402.4 eV and at higher energies. The theoretical spectrum of the relaxed FePc has two main peaks at 398.5 eV (with a shoulder at 399.1 eV) and at 399.8 eV,

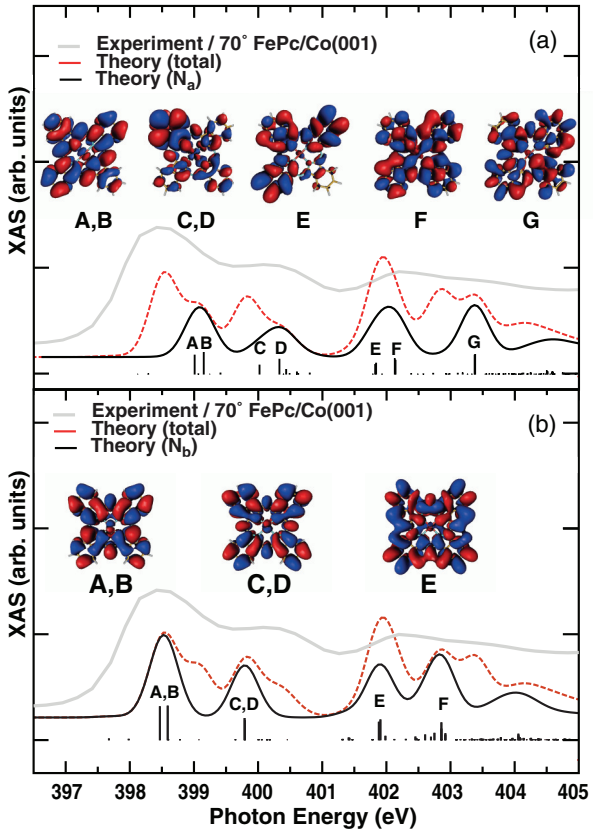

FIG. 11. (Color online) N K edge, detail. (a) Simulation of perpendicular polarization for N_a; (b) simulation of perpendicular polarization for N_b. The experimental spectrum in the quasiperpendicular set up at 70° is shown (grey thick line). The red dashed line is the total spectrum for the relaxed FePc. The bar graphs show the calculated oscillator strengths for N_a (a) and N_b (b).

a deep valley at 400.9 eV, followed by a succession of peaks at 401.9, 402.8, and 403.3 eV. Finally there is a smaller peak at 404.7 eV. For the symmetric molecule, one can observe a main peak at 398.7 eV, followed by a double peak at 400.0 and 400.5 eV. The valley is located at 401.3 eV. Another major peak is at about 402.5 eV, and a double peak follows at 403.7 and 404.1 eV. A low intensity shoulder is found at 405.2 eV.

Apart from small energy differences, both these simulations reproduce the general features of the experimental spectrum. The peaks are due to transitions of N 1s electrons into molecular orbitals with π^* character centered in both N_a and N_b. More information about the interaction with the surface can be extracted by the parallel polarization of Fig. 10(b). The experimental curve has a broad structure at 399 eV, and indistinguishable small peaks covering the whole region below the absorption edge. The theoretical simulation in the case of the symmetric FePc gives only two peaks at energies below the absorption edge. These peaks at 399.6 and 400.6 eV are due to the 1s excitation in a N_a atom into in-plane σ^* molecular orbitals formed by the hybridization of the Fe $3d_{x^2-y^2}$ with N 2p and C 2p. In contrast, the calculated spectrum for the relaxed molecule is much richer in structures at the lower energies, in agreement with the experimental spectrum of Fig. 10(b). This series of small resonances is due to the significant out-of-plane distortion of the relaxed molecule caused by the interaction with the surface. In the adsorbed, relaxed FePc, the π^* orbitals are not oriented exactly along the out-of-plane direction, but have components also in the plane of the molecule, and these components become visible in the measurements at parallel polarization. From the K edge theoretical and experimental results we can therefore conclude that in FePc/Co(001) there is a strong interaction of the molecule with the Co substrate which induces a distortion in the molecular structure. This effect is clearly visible in the parallel polarization of the NEXAFS N K-edge spectra, and is well reproduced by our simulations. In Fig. 11 we present the distinct contributions of the two nonequivalent N atoms of the distorted molecule to the simulation of the measurements at almost perpendicular polarization. The partial NEXAFS of N_a is shown in panel (a) and the partial NEXAFS of N_b is shown in panel (b), in comparison with the total theoretical curve and with the experiment. The main peaks are related to the isodensity surfaces for the final-state orbitals calculated by StoBe. Since the N_a atom is bound to the C atoms and the Fe atom (see Fig. 1), the individual π^* resonances are located at higher photon energies as compared to the N_b atom. The main observation is that the high intensity peaks are related to final states of π^* character mostly centered on the C atoms, and especially on the benzene C atoms, like for example in the orbitals C, D, and E of panel (a). The C atoms located on the benzene rings are also primarily responsible for the molecule/surface hybridization according to our calculations of the adsorption configuration. The asymmetry in the orbitals presented in Fig. 11 are due to the presence of the half core hole.

The almost perpendicular N K-edge NEXAFS spectrum of the FePc/O/Co of Fig. 9(b) presents two slightly more resolved peaks at 400.3 and 402.4 eV with respect to the equivalent features in the FePc/Co spectra. Similarly, the simulated spectrum of the symmetric molecule (Fig. 10) is characterized by slightly better distinguished peaks. This is a hint, confirmed also by our geometry relaxation calculations, that the FePc on the O-covered surface maintains a flat structure more similar to the gas phase molecule, and that the interaction with the surface is mostly mediated by the Fe atom in the molecule.

VII. CONCLUSIONS

The influence of an intermediate oxygen layer on the magnetic coupling between FePc molecules and a Co(001) film has been investigated by means of x-ray-absorption spectroscopy and DFT calculations. These investigations indicate a strong FM coupling of FePc with the bare Co substrate, which turns into an AF coupling if the surface is covered by 1/2 ML of oxygen. The oxygen adlayer causes also a weakening of the magnetic coupling between molecule and substrate, which leads to a stronger temperature dependence of the XMCD signal. By computing the coupling strengths of these two systems we reveal that the coupling energy on O/Co is reduced by a factor of 2 compared to the bare surface, which is in agreement with the experimental finding. From the investigation of the magnetization density, it turns out that the coupling mechanism on the oxidized surface is a 180° superexchange between Fe and Co via oxygen. This is similar

to the mechanism, which has been previously proposed for Fe OEP on O/Co.[7] On the bare Co surface, a mixture of direct exchange coupling between Fe and the underlying Co atom is observed, but in addition, the C rings of FePc contribute to the coupling. Very recently, a similar direct exchange coupling has been reported for Fe porphyrin on Co(001).[11] The four additional N atoms (N_b) play only a minor role in the coupling between molecule and substrate. The spin state seems to be unaffected by the O layer, i.e., with and without O, the FePc molecule is in an $S = 1$ spin state. Finally, our calculated angle-dependent NEXAFS match the experimental results very well. Due to the stronger interaction on the bare Co surface, the broader structures resemble the spectrum of the relaxed FePc, while the sharper structures on the O/Co surface fit the calculations for the free molecule.

ACKNOWLEDGMENTS

We thank the HZB-BESSY II staff for support during synchrotron beamtime, and acknowledge funding by BMBF (05 ES3XBA/5). The Swedish Research Council (VR) is acknowledged, as well as the Swedish National Infrastructure for Computing (SNIC) for providing computing time on the clusters Triolith at Linköping University and Lindgren at KTH, Stockholm. O.E. acknowledges support from VR, the KAW Foundation, eSSENCE, and the ERC (Project No. 247062 - ASD).

*david.klar@uni-due.de

[1] V. Dediu, M. Murgia, F. C. Matacotta, C. Taliani, and S. Barbarena, Solid State Commun. **122**, 181 (2002).
[2] L. Bogani and W. Wernsdorfer, Nat. Mater. **7**, 179 (2008).
[3] Z. H. Xiong, D. Wu, Z. V. Vardeny, and J. Shi, Nature (London) **427**, 821 (2004).
[4] A. Candini, S. Klyatskaya, M. Ruben, W. Wernsdorfer, and M. Affronte, Nano Lett. **11**, 2634 (2011).
[5] A. Scheybal, T. Ramsvik, R. Bertschinger, M. Putero, F. Nolting, and T. A. Jung, Chem. Phys. Lett. **411**, 214 (2005).
[6] H. Wende *et al.*, Nat. Mater. **6**, 516 (2007).
[7] M. Bernien *et al.*, Phys. Rev. Lett. **102**, 047202 (2009).
[8] M. Bernien *et al.*, Phys. Rev. B **76**, 214406 (2007).
[9] S. Bhandary, S. Ghosh, H. Herper, H. Wende, O. Eriksson, and B. Sanyal, Phys. Rev. Lett. **107**, 257202 (2011).
[10] S. Bhandary, O. Eriksson, and B. Sanyal, Sci. Rep. **3**, 3405 (2013).
[11] S. Bhandary *et al.*, Phys. Rev. B **88**, 024401 (2013).
[12] M. G. Betti *et al.*, J. Phys. Chem. C **114**, 21638 (2010).
[13] M.-E. Ragoussi *et al.*, Angew. Chem. Int. Ed. **51**, 4375 (2012).
[14] M. A. Loi *et al.*, J. Mater. Chem. **13**, 700 (2003).
[15] E. Annese, J. Fujii, I. Vobornik, G. Panaccione, and G. Rossi, Phys. Rev. B **84**, 174443 (2011).
[16] E. Annese, F. Casolari, J. Fujii, and G. Rossi, Phys. Rev. B **87**, 054420 (2013).
[17] M. Cinchetti *et al.*, Nat. Mater. **8**, 115 (2009).
[18] L. Margheriti *et al.*, Adv. Mater. **22**, 5488 (2010).
[19] A. Lodi Rizzini *et al.*, Phys. Rev. Lett. **107**, 177205 (2011).
[20] D. Klar *et al.*, Beilstein J. Nanotechnol. **4**, 320 (2013).
[21] M. Lackinger and M. Hietschold, Surf. Sci. **520**, L619 (2002).
[22] C. Bobisch, T. Wagner, A. Bannani, and R. Möller, J. Chem. Phys. **119**, 9804 (2003).
[23] A. Gerlach, F. Schreiber, S. Sellner, H. Dosch, I. A. Vartanyants, B. C. C. Cowie, T.-L. Lee, and J. Zegenhagen, Phys. Rev. B **71**, 205425 (2005).
[24] C. Stadler, S. Hansen, F. Pollinger, C. Kumpf, E. Umbach, T. L. Lee, and J. Zegenhagen, Phys. Rev. B **74**, 035404 (2006).
[25] H. Karacuban *et al.*, Surf. Sci. **603**, L39 (2009).
[26] C. Stadler, S. Hansen, I. Kröger, C. Kumpf, and E. Umbach, Nat. Phys. **5**, 153 (2009).
[27] Y. Wang, J. Kröger, R. Berndt, and W. Hofer, Angew. Chem. Int. Ed. **48**, 1261 (2009).
[28] X. Chen and M. Alouani, Phys. Rev. B **82**, 094443 (2010).
[29] H.-l. Fan, S.-l. Lei, J. Huang, and Q.-x. Li, Chin. J. Chem. Phys. **23**, 565 (2010).
[30] I. Kröger *et al.*, New J. Phys. **12**, 083038 (2010).
[31] I. Kröger, B. Stadtmüller, C. Kleimann, P. Rajput, and C. Kumpf, Phys. Rev. B **83**, 195414 (2011).
[32] B. Stadtmüller, I. Kröger, F. Reinert, and C. Kumpf, Phys. Rev. B **83**, 085416 (2011).
[33] C. M. Schneider, P. Bressler, P. Schuster, J. Kirschner, J. J. de Miguel, and R. Miranda, Phys. Rev. Lett. **64**, 1059 (1990).
[34] R. Nünthel *et al.*, Surf. Sci. **531**, 53 (2003).
[35] J. Hong, R. Q. Wu, J. Lindner, E. Kosubek, and K. Baberschke, Phys. Rev. Lett. **92**, 147202 (2004).
[36] C. Sorg, N. Ponpandian, M. Bernien, K. Baberschke, H. Wende, and R.Q. Wu, Phys. Rev. B **73**, 064409 (2006).
[37] X. Liu, T. Iimori, K. Nakatsuji, and F. Komori, Appl. Phys. Lett. **88**, 133102 (2006).
[38] G. Kresse and J. Furthmüller, Comp. Mater. Sci. **6**, 15 (1996).
[39] G. Kresse and D. Joubert, Phys. Rev. B **59**, 1758 (1999).
[40] S. L. Dudarev, G. A. Botton, S. Y. Savrasov, C. J. Humphreys, and A. P. Sutton, Phys. Rev. B **57**, 1505 (1998).
[41] S. Lach *et al.*, Adv. Func. Mater. **22**, 989 (2012).
[42] A. Mugarza, R. Robles, C. Krull, R. Korytár, N. Lorente, and P. Gambardella, Phys. Rev. B **85**, 155437 (2012).
[43] S. Grimme, J. Comput. Chem. **27**, 1787 (2006).
[44] C. Xu, J. S. Burnham, S. H. Goss, K. Caffey, and N. Winograd, Phys. Rev. B **49**, 4842 (1994).
[45] StoBe-deMon version 3.0 (2007), K. Hermann, L. G. M. Pettersson, M. E. Casida, C. Daul, A. Goursot, A. Koester, E. Proynov, A. St-Amant; D. R. Salahub, contributing authors: V. Carravetta, H. Duarte, C. Friedrich, N. Godbout, J. Guan, C. Jamorski, M. Leboeuf, M. Leetmaa, M. Nyberg, S. Patchkovskii, L. Pedocchi, F. Sim, L. Triguero, and A. Vela, http://www.fhi-berlin.mpg.de/KHsoftware/StoBe/index.html.
[46] B. Brena *et al.*, J. Chem. Phys. **134**, 074312 (2011).
[47] A. D. Becke, Phys. Rev. A **38**, 3098 (1988).
[48] J. P. Perdew, Phys. Rev. B **33**, 8822 (1986).
[49] W. Kutzelnigg, U. Fleischer, and M. Schindler, in *NMR Basic Principles and Progress* (Springer-Verlag, Berlin, Heidelberg, 1991), Vol. 23, pp. 165–262.
[50] L. Triguero, L. G. M. Pettersson, and H. Ågren, Phys. Rev. B **58**, 8097 (1998).

[51]L. T. O. Plashkevych, L. G. M. Pettersson, and H. Ågren, J. Electron Spectrosc. Relat. Phenom. **104**, 195 (1999).
[52]H. C. Herper, S. Bhandary, O. Eriksson, B. Sanyal, B. Brena (unpublished).
[53]S. Javaid *et al*., Phys. Rev. Lett. **105**, 077201 (2010).
[54]M. L. M. Rocco, K. H. Frank, P. Yannoulis, and E. E. Koch, J. Chem. Phys. **93**, 6859 (1990).
[55]T. Kroll, R. Kraus, R. Schönfelder, V. Yu. Aristov, O. V. Molodtsova, P. Hoffmann, and M. Knupfer, J. Chem. Phys. **137**, 054306 (2012).
[56]N. Haack, G. Ceballos, H. Wende, K. Baberschke, D. Arvanitis, A. L. Ankudinov, and J. J. Rehr, Phys. Rev. Lett. **84**, 614 (2000).